AD-A070 483 MARYLAND UNIV COLLEGE PARK DEPT OF PHYSICS AND ASTRONOMY F/G 20/9
PLASMA CONVECTION INSTABILITY IN AN INHOMOGENEOUS MAGNETIC FIEL--ETC(U)
1977 P OTTINGER, J GUILLORY, H LASHINSKY N00014-75-C-0309

UNCLASSIFIED PUB-77-107 NL

| OF |
AD
A070483

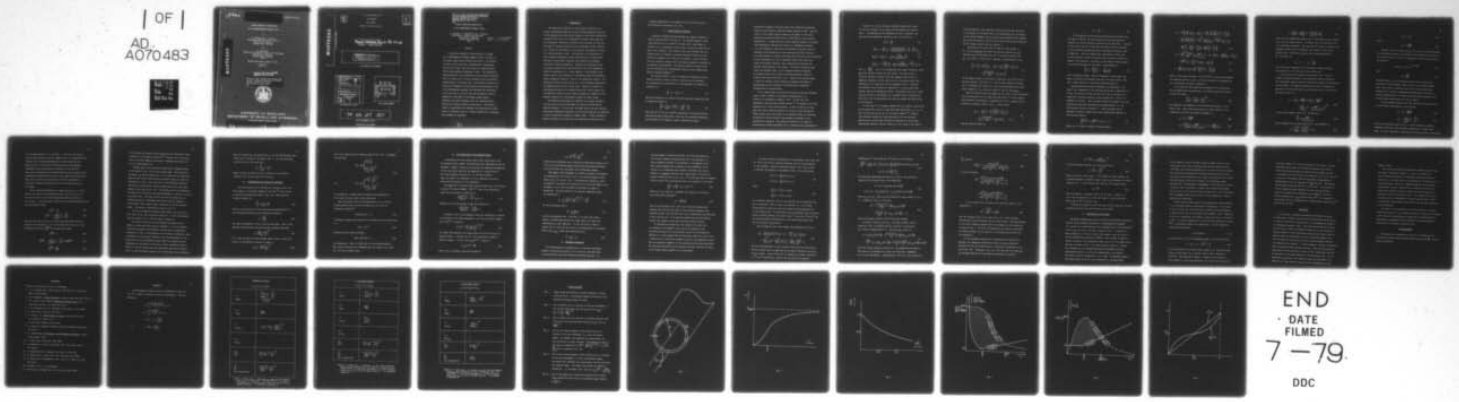

END
DATE FILMED
7-79
DDC

PREPRINT #710P002

PLASMA CONVECTION INSTABILITY

IN AN INHOMOGENEOUS MAGNETIC FIELD

by

P. Ottinger and J. Guillory
Department of Physics and Astronomy
University of Maryland
College Park, Maryland

and

H. Lashinsky
Institute for Physical Science and Technology
University of Maryland
College Park, Maryland
20742

Physics Publication Number 77-107

1977

Work on this report was supported by ONR Contract N00014-75-C-0309 and/or N00014-67-A-0239 monitored by NRL 6702.02.

UNIVERSITY OF MARYLAND
DEPARTMENT OF PHYSICS AND ASTRONOMY
COLLEGE PARK, MARYLAND

DDC PROCESSING DATA

PHOTOGRAPH

THIS SHEET

RETURN TO DDA-2 FOR FILE

II
LEVEL

1
INVENTORY

AD A070483

DDC ACCESSION NUMBER

Preprint 710P002, Physics Pub 77-107

DOCUMENT IDENTIFICATION

DISTRIBUTION STATEMENT A
Approved for public release;
Distribution Unlimited

DISTRIBUTION STATEMENT

Accession For
NTIS GRA&I
DDC TAB
Unannounced
Justification
By
Distribution/
Availability Codes
Dist. | Avail and/or special
A

DISTRIBUTION STAMP

DDC
RECEIVED
JUN 28 1979
D

DATE ACCESSIONED

79 06 27 311

DATE RECEIVED IN DDC

PHOTOGRAPH THIS SHEET

RETURN TO DDA-2

Work on this report was supported
by ONR Contract N00014-75-C-0309
and/or N00014-67-A-0239
monitored by NRL 6702.
02.

PLASMA CONVECTION INSTABILITY

IN AN INHOMOGENEOUS MAGNETIC FIELD

P. Ottinger, H. Lashinsky*, and J. Guillory
Department of Physics and Astronomy
University of Maryland
College Park, Maryland
20742

Abstract

A convection instability characteristic of plasmas in an inhomogeneous azimuthal magnetic field is treated in the linear stage and in nonlinear saturation. The analysis is done in such a way that collisional and collisionless limits can be taken, and these limits are displayed along with the more general intermediate result. The instability, known previously in the literature in its collision-dominated form,[1] is shown to be a "flute" instability with collisional modifications to the growth rate. The nonlinear saturation is analyzed by examining a finite amplitude restoring-force term in the differential equation that describes the instability. This term is due to the fact that the instability convects plasma into striations of the plasma column surface, modifying the density gradient until the restoring forces balance the pressure gradient driving force. The effects of finite ion gyroradius are displayed, and applications of this study to convection cells in a thermal plasma and to exploding wire plasmas are discussed.

I. INTRODUCTION

The conventional approach to evaluating the stability of a plasma configuration makes use of the so-called dispersion relation. In this approach one starts with a number of first-order differential equations, with time as the independent variable; these equations are essentially conservation relations which describe the time rate-of-change of physical quantities such as momentum, energy, density, etc. Points of equilibrium of the system are determined by setting the time derivatives to zero. The stability of an equilibrium is then evaluated by applying a small perturbation to the system and setting up "variational" equations which describe the temporal evolution of these perturbations. Typically one linearizes these variational equations and seeks solutions of the form $f(\underset{\sim}{x})\exp(i\omega t)$, where the frequency, ω, is a complex quantity. This procedure then usually leads to the formation of a determinant which, when expanded, forms an algebraic equation, which is the dispersion relation. The dispersion relation is then solved for ω, with stability depending on the imaginary parts of the various roots. While it is useful for determining the onset of an instability and the initial growth rate, the dispersion relation is not always convenient for analysis of the temporal evolution of a perturbation beyond the linear stage.

The problem of evaluating the stability of a plasma configuration can also be treated by what might be called the "differential--equation" approach. In this case, one again starts with the required first-order differential equations, but now these equations are combined to form a differential equation of higher order. In many problems of physical interest it is found that the conservation relations can be

a thermal plasma device is discussed in Sec. VI and the results of the work are discussed in Sec. VII.

II. LINEAR STABILITY ANALYSIS

Consider a plasma-filled gap between two coaxial cylinders of radius R and R+d, with d<<R (Fig. 1). An azimuthal magnetic field, which falls off as 1/R, exists in the gap; such a field might be produced, e.g., by passing a current along a conductor located at the axis of the cylinders. The surface of the inner cylinder acts as a plasma source, for example, by thermal ionization[1] while the outer cylinder is assumed to be a sink for the plasma. It will be shown that this system is unstable since the density gradient is parallel to the magnetic field gradient. The general problem is treated first and the collisional and collisionless limits are then compared with results obtained elsewhere.[1-3]

The two-fluid model is used to describe the plasma and the isothermal equation of state is used to close the set of equations. The quasineutrality approximation is also employed; the equation of continuity is

$$\frac{\partial n}{\partial t} + \nabla \cdot (n \underset{\sim}{V}_\alpha) = 0 \qquad (1)$$

where the subscript α=i,e denotes ions and electrons respectively and the momentum equation is

$$\frac{\partial \underset{\sim}{V}_\alpha}{\partial t} = \frac{q_\alpha}{m_\alpha}\left(\underset{\sim}{E} + \frac{\underset{\sim}{V}_\alpha \times \underset{\sim}{B}}{c}\right) - \frac{T_\alpha \nabla n}{m_\alpha n} - \frac{\underset{\sim}{V}_\alpha}{\tau_\alpha}, \qquad (2)$$

where τ_i^{-1} and τ_e^{-1} are the collision frequencies of neutrals with the ions and electrons respectively. Note that the convective derivative can be ignored if the magnetic field is sufficiently large.

expressed by algebraic relations rather than differential equations, because certain physical quantities remain constant in time. Thus the "order" of the system, which is equal to the number of first-order differential equations required for its description, can be reduced significantly. In many cases the overall equation reduces to a second-order differential equation with time as the independent variable. It is then possible to make use of the extensive literature that is available on the properties of these equations and their solutions. It is also possible to identify the terms which play the role of restoring forces, dissipation etc. and to determine factors that enter into linear and nonlinear behavior; these capabilities facilitate the physical interpretation of the results. The role of different time scales also becomes clear, so that standard methods of singular perturbation theory can be used in obtaining nonlinear solutions in which such time scales play a role. Finally, this approach makes it easier to evaluate various different techniques that might be employed when one is interested in stabilization of undesired instabilities by external means.

In the present paper the differential-equation approach described above is used to analyze an instability characteristic of a plasma in an inhomogeneous magnetic field. We show that this instability, which has been treated earlier,[1-3] is related to the flute instability in a fully ionized plasma. In Secs. II and III of this paper the linear stability analysis is carried out and interpreted. Finite Larmor radius corrections to the pressure tensor are discussed in Section IV, and in Section V the nonlinear saturation of the instability is analyzed. The possible relevance of the theory to exploding-wire plasma experiments and to convection-cell experiments in

Since d<<R, a local cartesian coordinate system with origin in the outer cylinder can be used as an approximation as shown in Fig. 1. Considering only the dependence on the x coordinate, one can write the steady-state solution of Eqs. (1) and (2) as

$$n^0(x) = \frac{Nx}{d} \tag{3}$$

$$\underset{\sim}{E}^0(x) = -\frac{\partial \phi^0}{\partial x}\,\hat{\underset{\sim}{e}}_x = \left(\frac{T_i(\Omega\tau)_e - T_e(\Omega\tau)_i}{e[(\Omega\tau)_e + (\Omega\tau)_i]}\right)\frac{\hat{\underset{\sim}{e}}_x}{x} \equiv \frac{E^0 d}{x}\,\hat{\underset{\sim}{e}}_x \tag{4}$$

$$\underset{\sim}{V}^0_{ex}(x) = \underset{\sim}{V}^0_{ix}(x) = -\frac{c}{eB}\left(\frac{T_i + T_e}{(\Omega\tau)_e + (\Omega\tau)_i}\right)\frac{\hat{e}_x}{x} \tag{5}$$

$$\underset{\sim}{V}^0_{ez}(x) = -\frac{(\Omega\tau)_e}{(\Omega\tau)_i}\,\underset{\sim}{V}^0_{iz} = \frac{c}{eB}\left(\frac{T_i + T_e}{(\Omega\tau)_e + (\Omega\tau)_i}\right)\frac{(\Omega\tau)_e}{x}\,\hat{\underset{\sim}{e}}_z \tag{6}$$

with $\Omega_\alpha \equiv \left|\frac{q_\alpha B}{m_\alpha c}\right|$. Here it is assumed that the change in magnetic field, $\underset{\sim}{B}_0$, across the gap is small and that n(0)=0. The flow in the -x direction (radially outward) across the magnetic field is due to ambipolar diffusion, and the motion in the z direction arises from a combination of the $\underset{\sim}{E}\times\underset{\sim}{B}$ drift and the diamagnetic drift. Although the gradient B drift drives the instability it is much slower than both the $\underset{\sim}{E}\times\underset{\sim}{B}$ and the diamagnetic drifts. The behavior near x=0 in these equations is due to the presence of a boundary layer of thickness on the order of the ion gyroradius, and does not present any difficulties in the analysis.

At this point it is normally assumed that the unstable oscillations in the system will occur on a time scale much slower than τ_i or τ_e, so that the inertial term in Eq. (2) is usually ignored.[1-4] However, that procedure reduces the resulting equation for the perturbed density from a second-order differential equation to a first-order differential equation, thereby losing one of the roots of the charac-

teristic equation. More important, keeping the inertial term leads to corrections to the growth rate of the instability and corrections to the critical magnetic field at which the instability first appears. The tables discussed at the end of this section show these corrections and the ranges in which they are important.

Retaining the inertial term, we take the cross product of Eq. (2) with $\underset{\sim}{b}=\underset{\sim}{B}_0/|\underset{\sim}{B}_0|$ and solve the resultant equation for $\underset{\sim}{V}_\alpha\times\underset{\sim}{b}$. Substituting this expression into Eq. (2) yields an equation for $\underset{\sim}{V}_{\alpha\perp}$ (the symbol "$\perp$" means that a component is perpendicular to $\underset{\sim}{b}$).

$$\left(\Omega_\alpha^2+\left(\frac{1}{\tau_\alpha}+\frac{\partial}{\partial t}\right)^2\right)\underset{\sim}{V}_{\alpha\perp}=-\left(\frac{1}{\tau_\alpha}+\frac{\partial}{\partial t}\right)\left(\frac{T_\alpha\underset{\sim}{\nabla}_\perp n}{m_\alpha n}+\frac{q_\alpha}{m_\alpha}\underset{\sim}{\nabla}_\perp\phi\right)$$
$$+\Omega_\alpha\left(\frac{q_\alpha T_\alpha(\underset{\sim}{b}\times\underset{\sim}{\nabla}n)}{em_\alpha n}+\frac{e}{m_\alpha}(\underset{\sim}{b}\times\underset{\sim}{\nabla}\phi)\right) \tag{7}$$

If the magnetic field is sufficiently large then $(1/\tau_\alpha+\partial/\partial t)^2$ can be ignored compared to Ω_α^2 in Eq. (7), but all other terms are retained. If it is assumed that $\partial/\partial y=0$ (i.e., that the perturbations are azimuthally symmetric), $V_{\alpha y}$ can be set equal to zero, so that $\underset{\sim}{V}_\alpha=\underset{\sim}{V}_{\alpha\perp}$.

When the inertial terms are ignored at the onset of the calculations, the time derivatives on the right hand side of Eq. (7) do not appear. This procedure is equivalent to assuming that $\omega<<1/\tau_\alpha$, whereas Eq. (7) extends the frequency range to $\omega\gtrsim 1/\tau_\alpha$. Thus we have

$$\underset{\sim}{V}_{\alpha\perp}=-\frac{1}{\Omega_\alpha^2}\left(\frac{1}{\tau_\alpha}+\frac{\partial}{\partial t}\right)\left(\frac{T_\alpha\underset{\sim}{\nabla}_\perp n}{m_\alpha n}+\frac{q_\alpha}{m_\alpha}\underset{\sim}{\nabla}_\perp\phi\right)$$
$$+\frac{1}{\Omega_\alpha}\left(\frac{q_\alpha T_\alpha(\underset{\sim}{b}\times\underset{\sim}{\nabla}n)}{em_\alpha n}+\frac{e}{m_\alpha}(\underset{\sim}{b}\times\underset{\sim}{\nabla}\phi)\right)\qquad\alpha=i,e \tag{8}$$

and this relation holds for

$$\Omega_\alpha >> \frac{1}{\tau_\alpha} \simeq \omega \tag{9}$$

If one considers electrostatic perturbations which depend only on x and z, then Eq. (8) can be substituted into the continuity equation (1), and the resulting equation can be linearized. The next to last term in Eq. (8) is the only term which does not contribute to the continuity equation when B_0 is considered a constant (since $\underset{\sim}{\nabla}\cdot(\underset{\sim}{b}\times\underset{\sim}{\nabla}n')=0$). Thus the leading order contribution of this term to the linearized continuity equation results from the presence of a magnetic field gradient. The effect of the magnetic field gradient is introduced through this term which is approximated by

$$\frac{cT_\alpha}{e}\,\underset{\sim}{\nabla}\cdot\left(\frac{\underset{\sim}{b}\times\underset{\sim}{\nabla}n'}{B_0}\right) \simeq -\frac{cT_\alpha}{eRB_0}\frac{\partial n'}{\partial z}\,. \tag{10}$$

where $\partial/\partial x[B_0(\underset{\sim}{r})]\simeq -1/RB_0$. Here the assumption $d<<R$ has been used. Again if B_0 were truly constant then this term would vanish. Note that a prime signifies a first-order perturbed quantity.

Following the method used by Kadomtsev and Nedospasov,[4] and Simon[5] the x dependence of the perturbed quantities is expressed by a Fourier sine series in which only the first term is retained; the linearized continuity equation is then averaged over x from 0 to d weighted by $\sin(\pi x/d)$. This procedure yields two coupled first order differential equations involving the perturbed density, n', and the perturbed electric potential, ϕ'. These equations can be combined to obtain a single second order differential equation in the perturbed density:

$$\frac{d^2n'(t)}{dt^2} + A_1\frac{dn'(t)}{dt} + A_2n'(t) = 0 \tag{11}$$

where now n' is only a function of time and where

$$A_1 = +\frac{1}{\beta}\left\{+\frac{Bd}{8c}\left(\frac{1}{(\Omega\tau)_e}+\frac{1}{(\Omega\tau)_i}\right)+\frac{k^2d}{8e}\frac{(T_i\tau_i+T_e\tau_e)}{(\Omega\tau)_i(\Omega\tau)_e}\left(1+\frac{2\pi\varepsilon_1}{k^2d^2}\right)\right.$$
$$+\frac{k^2d}{8e}\frac{(T_e\tau_i-T_i\tau_e)}{(\Omega\tau)_e(\Omega\tau)_i}+\frac{\pi\varepsilon_1E^0}{4}\frac{(\tau_e-\tau_i)}{(\Omega\tau)_e(\Omega\tau)_i}+\frac{ikd\varepsilon_2E^0}{4}\left(\frac{1}{\Omega_i}+\frac{1}{\Omega_e}\right)$$
$$\left.-\frac{ik}{4e}\left(\frac{T_i}{\Omega_i}-\frac{T_e}{\Omega_e}\right)\left(1-\frac{2\pi\varepsilon_1}{k^2d^2}\right)-\frac{ikd}{8eR}\left(\frac{T_i}{\Omega_e}-\frac{T_e}{\Omega_i}\right)\right\} \tag{12}$$

$$A_2 = +\frac{1}{\beta}\left\{\frac{k^2(T_i+T_e)}{4eRK^2}\left(\frac{dRK^4}{2k^2(\Omega\tau)_i(\Omega\tau)_e}-1\right)-\frac{ik}{4e}\left(1-\frac{d}{2R}\right)\left(\frac{T_i}{(\Omega\tau)_i}-\frac{T_e}{(\Omega\tau)_e}\right)\right.$$
$$\left.+\frac{ikdE^0}{4}\left(\varepsilon_2+\frac{2\pi\varepsilon_1}{k^2d}\right)\left(\frac{1}{(\Omega\tau)_e}+\frac{1}{(\Omega\tau)_i}\right)\right\} \tag{13}$$

$$\beta = \left\{\frac{Bd}{8c}\left(\frac{1}{\Omega_e}+\frac{1}{\Omega_i}\right)+\frac{k^2d}{8e}\frac{(T_i+T_e)}{\Omega_e\Omega_i}\left(1-\frac{2\pi\varepsilon_1}{k^2d^2}\right)\right\} \tag{14}$$

Here k is the axial wavenumber and $K^2=\pi^2/d^2+k^2$ is the total wavenumber. The numerical factors ε_1 and ε_2, which are obtained by averaging over the x coordinate, are given in Appendix I.

Since these are very complicated expressions, the coefficients will be simplified by specializing to the case $T_i=T_e\equiv T$ and by using the Spitzer[6] result

$$\frac{(\Omega\tau)_i}{(\Omega\tau)_e}=\frac{(\tau/m)_i}{(\tau/m)_e}\simeq\left(\frac{m_e}{m_i}\right)^{1/2}<<1\ . \tag{15}$$

For simplicity the remainder of this section will pertain to this special case. Under these conditions A_1, A_2 and β reduce to (η is a numerical factor and is defined in Appendix I)

$$A_1=\frac{1}{\tau_i}+\frac{2i\eta kTc}{eBd} \tag{16}$$

$$A_2=\frac{1}{\beta}\left\{\frac{k^2T}{2eRK^2}\left(\frac{dRK^4}{2k^2(\Omega\tau)_i(\Omega\tau)_e}-1\right)+\frac{i\eta kT}{4e(\Omega\tau)i}\right\} \tag{17}$$

$$\beta = \left\{ \frac{Bd}{8c\Omega_i} + \frac{K^2 dT}{8e\Omega_i \Omega_e} \left(1 - \frac{2\pi\varepsilon_1}{K^2 d^2} \right) \right\} \simeq \frac{Bd}{8c\Omega_i} \tag{18}$$

where the last approximate equality in Eq. (18) holds as long as $K^2 r_i^2 < 1$ (r_i is the ion Larmor radius). In Section IV we will show that this is a reasonable assumption. Also note that E^0, which is related to the ambipolar electric field through Eq. (4), reduces to T/e in this special case. In addition the axial drift velocities given by Eq. (6) reduce to

$$V_{iz} \simeq 0 \quad ; \quad V_{ez} \simeq \frac{2Tc}{eBx}$$

For the ions the diamagnetic drift essentially cancels the $\underset{\sim}{E}_a \times \underset{\sim}{B}$ drift whereas for the electrons the two drifts add.

Since A_1 and A_2 are complex, the solution of Eq. (11) will exhibit oscillatory behavior in the laboratory frame of reference. This oscillatory behavior results from the drift motion of the electron and ion fluids. The complex characteristic roots of differential equation (11) with coefficients A_1 and A_2 given by Eqs. (16) and (17) are easily found to be

$$\omega = -\left(\frac{1}{2\tau_i} + \frac{i\eta kTc}{eBd} \right) \pm \left[\left(\frac{1}{2\tau_i} - \frac{i\eta kTc}{eBd} \right)^2 + \frac{4k^2 T}{K^2 dRm_i} \left(1 - \frac{dRK^4}{2k^2 (\Omega\tau)_e (\Omega\tau)_i} \right) \right]^{1/2} \tag{19}$$

If the critical magnetic field, B_c, is defined as

$$\frac{B_c^2}{B^2} = \frac{dRK^4}{2k^2 (\Omega\tau)_e (\Omega\tau)_i} , \tag{20}$$

then for $B_c^2/B^2 \gtrsim 1$ the two roots given in Eq. (19) simplify to

$$\omega_1 \simeq \frac{4\tau_i k^2 T}{K^2 dRm_i} \frac{(1 - B_c^2/B^2)}{(1 + \omega_0^2 \tau_i^2)} + i\omega_0 \tag{21}$$

$$\omega_2 \simeq -\frac{1}{\tau_i} \tag{22}$$

where

$$\omega_0 \equiv -\frac{2\eta kTc}{eBd} \tag{23}$$

From Eq. (19) it is clear that ω_0, the part of ω_1 which determines the oscillation frequency, is related to the average drift velocity of the electron fluid, so that the z dependence of the perturbation may be written as

$$n_1(x,z,t) = n_1(x,t)e^{ik(z-v_D t)} \tag{24}$$

with

$$v_D \equiv \frac{2\eta Tc}{eBd} \tag{25}$$

The second mode, ω_2, can be associated with the ions, which are stationary in the laboratory frame, so that ω_2 is a purely damped mode. This result is similar to the case of the universal overstability of a resistive, inhomogeneous plasma where one mode is a purely growing mode in the frame drifting with the electrons, and the other mode drifting with the ions is damped.[7]

If one transforms equation (11) into the frame drifting with the electron fluid, coefficients A_1 and A_2 become

$$A_1 = \frac{1}{\tau_i} - \frac{2i\eta kTc}{eBd} \tag{26}$$

$$A_2 = -\frac{4k^2T}{m_i dRK^2}\left(1 - \frac{B_c^2}{B^2}\right) \tag{27}$$

Now if A_1 were merely equal to $1/\tau_i$, it would represent a positive dissipation term and could not lead to instability. On the other hand, A_2, which represents a restoring force term, can lead to instability

if it becomes negative (i.e., if $B>B_c$). In fact Eq. (11) with A_1 real and positive and A_2 real and negative will be recognized as the equation for an inverted pendulum and it can be shown that the general class of "convection" instabilities such as the Benard instability can be described by an equation of this form.[8,9] This class of instabilities is characterized by purely growing "zero-frequency" perturbations which arise from a negative restoring force. This present problem is very similar in that the instability is driven by a negative restoring force, but more general since A_1 is complex.

For the collision dominated case, where $\omega_0 << \gamma \lesssim 1/\tau_i$, ($\gamma$ is the growth rate) and in the collisionless limit ($\omega_0, \gamma >> 1/\tau_i$) Eq. (11) can take the form of the inverted pendulum equation with both A_1 and A_2 real. In the laboratory frame for this collision dominated case the coefficients become

$$A_1^{coll} \simeq \frac{1}{\tau_i} \tag{28}$$

$$A_2^{coll} \simeq -\frac{4k^2T}{m_i dRK^2}\left(1 - \frac{B_c^2}{B^2}\right) \tag{29}$$

Here the drift motion occurs on a time scale much slower than the growth of the instability. For the collision free case, in a frame drifting with velocity V_D^{FREE} the coefficients become

$$A_1^{FREE} \simeq 0 \tag{30}$$

$$A_2^{FREE} \simeq -\frac{4k^2T}{m_i dRK^4}\left(1 - \frac{B_c^2}{B^2}\right) + (kV_D^{FREE})^2 \tag{31}$$

$$V_D^{FREE} = \frac{\eta Tc}{eBd} \tag{32}$$

In both cases the general results derived for the "convection" type instability can be applied directly.[8,9] From Eq. (31) it is clear that the critical magnetic field must be redefined (see Table III) for the collisionless case.

Working again in the laboratory frame Table I summarizes some of the results of Eq. (19) for the unstable mode. The oscillation frequency, ω_0, and the growth rate, γ, are listed for the cases with $B \gtrsim B_c$ and with $B_c << B \to \infty$, where B must be greater than B_c in order for instability to occur. Note that even in the laboratory frame the instability is essentially a purely growing mode in the very large magnetic field limit ($\omega_0 \simeq 0$, $\gamma > 0$). The growth rate of the instability is plotted as a function of the axial wavenumber, k, in Fig. 2, for the case where $B >> B_c$. From this plot we see that the growth rate is largest when $k \gtrsim \pi/d$. Wavenumbers much larger than π/d should be stabilized by finite Larmor radius corrections to the ion pressure tensor. This point is discussed in detail in Sec. IV.

In the low frequency collisional limit where $1/\tau_i >> |\omega| = |\omega_r + i\gamma|$, the results of Eq. (19) are found in Table II. In the collisionless limit the results of Eq. (19) are listed in Table III.

The results listed for the low frequency collisional limit (Table II) agree with those found by Timofeev.[1] It is not possible to directly establish from Timofeev's results which collisionless instability, if any, is the analog of the collisional instability since he assumes $1/\tau_i >> |\omega| = |\omega_0 + i\gamma|$; however, since the expression for the growth rate in the collisionless limit (Table III) agrees with the expression for the growth of this type of flute instability found by Krall,[3] it can be inferred that the instability described in Tables I and II is the collisional analog of the collisionless flute instability.

Note that when $B>>B_c$, the growth rate, γ_0, for the collisionless case (Table III) is related to the growth rate, γ_c, for the collisional case (Table II) in the usual way:

$$\gamma_c = \frac{\gamma_0^2}{\nu_{coll}} = \gamma_0^2 \tau_i \ .$$

Figure 3 shows the growth rate as a function of the collision frequency, τ_i^{-1}, for the case $k>>\pi/d$ and $B>>B_c$.

III. INTERPRETATION OF INSTABILITY CRITERION

The interpretation of the instability criterion is not to be found simply in collisional damping of the mode,[10] as one can see by taking the collisionless limit of Eq. (19). This gives the condition (Table III):

$$\frac{r_i^2}{d^2} < \left(\frac{2}{\pi^2 \eta^2}\right)\left(\frac{d}{R}\right) \tag{33}$$

which is the condition for finite gyroradius stabilization[11] of the interchange instability with driving acceleration

$$g = \frac{v_{thi}^2}{2\eta^2 R} \tag{34}$$

and typical wavenumber $k \sim \pi/d$, as found in this paper. This is the dominant criterion until collisions become frequent enough that

$$\tau_i \lesssim \frac{2Kd}{\eta k v_{thi}} \left(\frac{m_e}{m_i}\right)^{1/4} \tag{35}$$

i.e., until the mean free path becomes shorter than d. When this occurs, the instability criterion is (Table I)

$$(\Omega\tau)_i^2 > \frac{2\pi^2 R}{d} \left(\frac{m_e}{m_i}\right)^{1/2} \tag{36}$$

for $k \sim \pi/d$, rather than the condition given in Eq. (33). In summary, one must have

$$d/R > \text{Max} \left\{ \frac{\pi^2 \eta^2}{2} \frac{r_i^2}{d^2}, \frac{2\pi^2}{(\Omega\tau)_i^2} \left(\frac{m_e}{m_i}\right)^{1/2} \right. \tag{37}$$

i.e.,

$$d/R > \text{Max} \left\{ \left(\frac{\pi^2 \eta^2}{2} \frac{r_i^2}{R^2}\right)^{1/3}, \frac{2\pi^2}{(\Omega\tau)_i^2} \left(\frac{m_e}{m_i}\right)^{1/2} \right.$$

for instability. Steeper density gradients are stabilized by finite mean free path and/or finite gyroradius.

When the magnetic field is self-generated, as in a current-carrying plasma pinch, one should compare Eq. (37) with the instability condition[12]

$$-d(\ell nP)/d(\ell nr) > 2\gamma \tag{38}$$

(γ=adiabatic exponent and should not be confused with the growth rate), i.e.,

$$d/R < (2\gamma)^{-1} , \tag{39}$$

obtained from the energy principle

$$\delta P \delta U + \frac{\gamma P}{U} (\delta U)^2 < 0 \tag{40}$$

for instability. (Here $U \equiv \int d\ell/B$ and P is the plasma pressure.) This latter condition sets a maximum value for unstable d's, while Eq. (37) sets a minimum value.

IV. FLR CORRECTIONS TO THE PRESSURE TENSOR

The addition of finite Larmor radius (FLR) corrections to the ion pressure tensor renders the mathematics very cumbersome and was not attempted. However, insight can be obtained by comparing the magnitude of such correction terms with the magnitude of a typical term in the linear analysis of Section II. If the FLR correction terms are found to be significant in this comparison, one would expect FLR stabilization of the instability.

The magnitude of a typical FLR correction term to Eq. (2) is given by $r_i^2\Omega_i/4\ S^2V$, where $S^2=\text{MAX}(k,\ \pi^2/d^2)$.[13] Thus in the collisional regime FLR corrections are important if

$$\frac{(r_i^2\Omega_i S^2 V/4)}{(V/\tau_i)} = \frac{S^2 r_i^2}{4}\,(\Omega\tau)_i \gtrsim 1 \tag{41}$$

Similarly in the collisionless regime the condition is

$$\frac{(r_i^2\Omega_i S^2 V/4)}{(V/|\omega|)} = \frac{s^2 r_i^2 \Omega_i}{4|\omega|} \gtrsim 1 \tag{42}$$

In Figure 4 the critical magnetic field for instability is plotted as a function of the axial wavenumber, k, for the collisional regime. Here $(\Omega\tau)_i^{\text{crit.}}$ is given by

$$(\Omega\tau)_i^{\text{crit}} = \frac{K^2R}{k}\left[\frac{d}{2R}\left(\frac{m_e}{m_i}\right)^{1/2}\right]^{1/2} \tag{43}$$

The dashed line separates the regions where the FLR corrections are large and small. A similar plot for the collisionless regime is shown in Figure 5. In this case $(\Omega_i\tau_N)^{\text{crit.}}$ is given by

$$(\Omega_i\tau_N)^{\text{crit}} = \frac{Kd}{\pi} \tag{44}$$

where τ_N is a convenient time scale defined by

$$\tau_N = \frac{2}{\eta}\left(\frac{m_i d^2}{T}\,\frac{d}{\pi^2 R}\right)^{1/2} \tag{45}$$

Unlike the collisionless case, collisional stabilization dominates for $k<\pi/d$ in the collisional regime, whereas FLR stabilization dominates for $k>\pi/d$ in both the collisional and collisionless regimes.

The largest axial wavenumber, k_L, which is unstable is determined by evaluating Eq. (41) (or Eq. (42)) at the critical magnetic field given by Eq. (43) (or Eq. (44)). This marginally unstable k_L value corresponds to the point of intersection of the solid and dashed curves in Figure 4 (or 5), and the shaded area denotes the region of instability. The FLR corrections can actually completely quench the instability if

$$\frac{\pi}{d} > \frac{1}{r_i}\left(\frac{32\, r_i^2}{Rd}\left(\frac{m_i}{m_e}\right)^{1/2}\right)^{1/6} \equiv \frac{\alpha^{1/6}}{r_i} \tag{46}$$

for the collisional case or

$$\frac{\pi}{d} > \frac{2}{(Rr_i^2)^{1/3}} \tag{47}$$

for the collisionless case. From this it is clear that Figure 2 should be modified particularly for large values of k where FLR stabilization is most important. In fact the curve in Figure 2 should fall off such that the value of k corresponding to the maximum growth rate, k_{max}, should fall between $\frac{\pi}{d}$ and k_L.

$$\frac{\pi}{d} < k_{max} < k_L \tag{48}$$

IV. NONLINEAR SATURATION

The understanding and identification of nonlinear mechanisms capable of limiting the growth of the instability described above is facilitated by using the differential-equation approach. It

has been argued in connection with Eq. (11) that the instability arises from a negative restoring force due to the presence of a density gradient parallel to the gradient of the magnetic field. This feature suggests that saturation of the instability can be obtained from a mechanism that provides a nonlinear term corresponding to a positive restoring force large enough to overcome the negative restoring force in Eq. (11). It can be shown that the simplest term that meets this specification leads to an equation of the form[8]

$$\frac{d^2y}{dt^2} + A_1 \frac{dy}{dt} + A_2 y + A_3 y^3 = 0 \qquad (49)$$

where $A_1>0$, $A_3>0$ and $A_2<0$. Evidently this equation is satisfied by the saturation amplitude[8]

$$y_s = \sqrt{|A_2/A_3|} \qquad (50)$$

Since the coefficients in Eq. (49) are all real this quasilinear analysis will strictly only apply to the collision dominated case described in Eqs. (28) and (29), and to the collisionless case described in Eqs. (30) and (31); it is expected however that the more general problem with complex coefficients would have similar results.

In considering the physics of the problem it is noted that the gradient of the magnetic field can not be affected by the instability because of the electrostatic nature of the instability. Therefore it is anticipated that the saturation effect will arise from a modification of the density gradient caused by the instability itself. Once the nonlinear component of the restoring force has been identified the saturation amplitude can be calculated from Eq. (50) and its effect on the linear density gradient can be determined.

In order to derive an expression for the nonlinear term in Eq. (49), Eq. (8) is used in the continuity equation, which is not linearized in this analysis. Again an expression similar to Eq. (10) is used to describe the gradient in the magnetic field. If we first write

$$\begin{aligned} n(x,z,t) &= n^0_{NL}(x)+n'(x,z,t) \\ \phi(x,z,t) &= \phi^0_{NL}(x)+\phi'(x,z,t) \end{aligned} \tag{51}$$

where

$$\begin{aligned} n^0_{NL}(x) &= n^0(x) + \delta n^0(x) \\ \phi^0_{NL}(x) &= \phi^0(x) + \delta\phi^0(x) \end{aligned} \tag{52}$$

the continuity equations (one for each species) can be integrated over the z coordinate.[9] Here n' and ϕ' are periodic in z in the frame drifting with the electron fluid and represent the perturbation due to the unstable mode. A time average is not appropriate since the perturbation is purely growing in the drift frame.[1] Note that δn^0 and $\delta\phi^0$ are the average nonlinear modifications to the equilibrium density and electric potential respectively.

After integration over z the steady state equations are (α=i,e)

$$\left\langle \underset{\sim}{\nabla} \cdot \left[\frac{T_\alpha}{\Omega_\alpha} \frac{n'}{n^{02}} \frac{\partial n'}{\partial t} \underset{\sim}{\nabla} n^0 + en' \underset{\sim}{b} \times \underset{\sim}{\nabla}\phi' - \frac{q_\alpha n'}{\Omega_\alpha} \left(\frac{1}{\tau_\alpha} + \frac{\partial}{\partial t} \right) \underset{\sim}{\nabla}\phi' \right.\right.$$
$$\left.\left. - \frac{q_\alpha n^0}{(\Omega\tau)_\alpha} \underset{\sim}{\nabla}\delta\phi^0 - \frac{q_\alpha \delta n^0}{(\Omega\tau)_\alpha} \underset{\sim}{\nabla}\phi^0 \right] \right\rangle_z + \frac{q_\alpha T_\alpha}{e(\Omega\tau)_\alpha} \frac{\partial^2 \delta n^0}{\partial x^2} = 0 \tag{53}$$

The only time dependence in this equation arises from the drift motion since in steady state the amplitude has saturated; therefore $\omega=\omega_0+i\gamma=\omega_0$ in what follows. Since δn^0 and $\delta\phi^0$ are assumed to be small corrections to n^0 and ϕ^0 respectively, terms of the form $\delta n^0 \delta\phi^0$ are ignored.

Eliminating $\delta\phi^0$ and solving for δn^0 results in the equation

$$\frac{\partial^2 \delta n^0}{\partial x^2} = \frac{1}{T_e+T_i} \left\langle \underset{\sim}{\nabla} \cdot \left[(T_e\tau_e+T_i\tau_i) \frac{n'}{n_{02}} \frac{\partial n'}{\partial t} \underset{\sim}{\nabla} n^0 + e((\Omega\tau)_i+(\Omega\tau)_e) n' \underset{\sim}{b}\times\underset{\sim}{\nabla}\phi' \right.\right.$$

$$\left.\left. + en'(\tau_e-\tau_i)\underset{\sim}{\nabla}\left(\frac{\partial\phi'}{\partial t}\right) \right] \right\rangle_z \tag{54}$$

The following expressions are used for n' and ϕ' (the subscript s signifies the saturated value of the amplitude)

$$n'(x,z,t) = n'_s \sin(kz-\omega_0 t)\sin\left(\frac{\pi x}{d}\right)$$

$$\phi'(x,z,t) = [\phi'_{s,s}\sin(kz-\omega_0 t) + \phi'_{s,c}\cos(kz-\omega_0 t)]\sin\left(\frac{\pi x}{d}\right) \tag{55}$$

where $\phi'_{s,s}$ and $\phi'_{s,c}$ allow for the difference in phase between n' and ϕ'. Solving Eq. (54) for δn^0 yields

$$\delta n^0 = \frac{e[(\Omega\tau)_e+(\Omega\tau)_i]}{T_e+T_i} \left(\frac{kd}{8\pi}\right) n'_s \phi'_{s,c} \sin\left(\frac{2\pi x}{d}\right)$$

$$+ \frac{e(\tau_i-\tau_e)}{T_e+T_i} \left(\frac{\omega_0}{8}\right) n'_s \phi'_{s,c} \left(\cos\left(\frac{2\pi x}{d}\right) - 1\right) \tag{56}$$

where the boundary condition $\delta n^0(d)=0$ has been invoked.

In order to relate n'_s and $\phi'_{s,c}$, the same procedure, used to obtain Eq. (53), is repeated with the exception of multiplying by n' before integrating over z. The resulting equation is

$$0 = (T_e+T_i) n'^2_s \sin^2\left(\frac{\pi x}{d}\right) - \left(\frac{(\Omega\tau)_e+(\Omega\tau)_i}{K^2}\right) \left(\frac{ekN}{d}\right) n'_s \phi'_{s,c} \sin^2\left(\frac{\pi x}{d}\right)$$

$$- \frac{e\omega_0 N}{d} (\tau_e-\tau_i) n'_s \phi'_{s,c} x \sin^2\left(\frac{\pi x}{d}\right) + \left(\frac{\tau_e-\tau_i}{K^2}\right)\left(\frac{e\omega_0 N\pi}{d^2}\right) n'_s \phi'_{s,c} \sin\left(\frac{\pi x}{d}\right)\cos\left(\frac{\pi x}{d}\right) \tag{57}$$

As in the linear analysis of Section II, the appropriate procedure at this point is to average over x since the functional dependence on x is only approximate. Integrating Eq. (57) over x and solving for

$\overline{\phi'_{s,c}}$ obtains

$$\overline{n'_s\phi'_{s,c}} = \frac{d(T_e+T_i)\overline{n'^2_s}}{eNk\left(\frac{(\Omega\tau)_e+(\Omega\tau)_i}{K^2} + \frac{\omega_0 d(\tau_e-\tau_i)}{4k}\right)} \tag{58}$$

so that δn^0 becomes

$$\delta n^0 = \frac{d^2\overline{n'^2}[(\Omega\tau)_e+(\Omega\tau)_i]\sin(\frac{2\pi x}{d})}{8\pi N\left(\frac{(\Omega\tau)_e+(\Omega\tau)_i}{K^2} + \frac{\omega_0 d}{4k}(\tau_e-\tau_i)\right)} \tag{59}$$

$$+ \frac{\omega_0\overline{n'^2}d(\tau_i-\tau_e)\left(\cos(\frac{2\pi x}{d})-1\right)}{8kN\left(\frac{(\Omega\tau)_e+(\Omega\tau)_i}{K^2} + \frac{\omega_0 d}{4k}(\tau_e-\tau_i)\right)}$$

If one considers the case where $k=\pi/d$ and $T_e \simeq T_i$, then Eq. (59) simplifies to

$$\delta n^0 = \frac{\overline{\pi(n'_s)^2}}{4N}\sin(\frac{2\pi x}{d}) \tag{60}$$

Here the assumption that $\omega << \Omega_\alpha$, used in Eq. (7), is also invoked, although here ω_0 may be shifted from the linear value. This modification of the initial density gradient due to the presence of the instability is shown in Fig. 6. Note that the modification is such as to decrease the density gradient in the interior of the plasma and thus shut off the instability.

If this nonlinear mechanism is incorporated into the previous analysis, the significant modification arises from the additional nonlinear term in the restoring force, resulting in an equation of the form of Eq. (49). Using Eqs. (13), (14), (50) and (60), one finds that the saturated amplitude of the density perturbation is given by

$$n_s' = \frac{2N}{\pi}\left(1 - \frac{2\pi^2 R}{d(\Omega\tau)_e(\Omega\tau)_i}\right)^{1/2} \tag{61}$$

In the collisional limit Eq. (61) can be written as

$$n_s' = \frac{2N}{\pi}\left(1 - \frac{B_c^2}{B^2}\right)^{1/2} \tag{62}$$

which is valid as long as $B \gtrsim B_c$. If B becomes too large, however, the nonlinear analysis is somewhat suspect, since n_s' was assumed to be small compared to N. In the collisionless limit Eq. (61) simply becomes

$$n_s' = \frac{2N}{\pi} \tag{63}$$

Here the analysis is somewhat suspect for all $B > B_c$. However it is clear that the amplitude can grow much larger in the collisionless case, than in the collisional case.

It should be pointed out that there may be other important nonlinear processes which have not been included in this model.

VI. EXPERIMENTAL APPLICATIONS

The plasma configuration used as a basis for the present instability analysis can be realized physically in an experimental arrangement that exploits the "vapor-pressure" mode sometimes used in the Q-machine.[16] In this case the role of the inner cylinder in Fig. 1 is played by a metal cylinder of a refractory metal like tungsten, which is heated to an electron-emitting temperature (2000°K). This cylinder is used for thermal ionization of an appropriate vapor and acts as the plasma source. The outer cylinder in Fig. 1 is a heat-resistant dielectric cylinder. This cylinder acts as a plasma sink since the outwardly drifting plasma which reaches it is lost by recombination at the surface. The annular space is flooded with C_s or K vapor. An azimuthal magnetic field which falls off as 1/r can be produced in a straightforward

way by passing a current through a single straight conductor along the cylinder axis, and calculations show that the required fields (10^2-10^3g) can be produced conveniently by conventional power sources. The time and space dependence of relevant plasma quantities such as the density can be measured by wall probes installed so as to be flush with the surface of the outer cylinder, thus minimizing plasma perturbations. An experimental arrangement of this kind is of interest in that it would be possible to observe the time-space development and structure of the convection cells characteristic of the instability. This arrangement would also be useful for the evaluation of various stabilization techniques.

Another possible application of the formalism for this instability is to the plasma formed by exploding-wire discharges. In the corona of such a plasma, one can have parallel, inwardly directed gradients of plasma density and of the azimuthal self magnetic field. Depending on the local temperature, the plasma at these radii may be collisional or not. At typical temperatures of order 200 eV and densities of order 10^{19}, collisionless dynamics are appropriate. At this temperature, deuterium has gyroradius

$$r_i(\text{cm}) \sim 2/B(\text{kG}) \ . \tag{64}$$

The self field can be in the megagauss range, so that the condition

$$B > B_c, \quad \text{i.e.,} \quad \left(\frac{r_i}{d}\right)^2 << \frac{d}{R} \tag{65}$$

can be satisfied for low-atomic number plasma (e.g., deuterium) even when d is quite small (e.g., density falloff over a distance of $d \sim 10^{-2}$cm.) The formation of beads, or ripples in the radius, of such plasmas is a well-known phenomenon and is much more violent for

low atomic numbers.[14] If this instability is the cause, a typical wavelength on the order $k \sim \pi/d$ should be expected, since finite Larmor radius effects reduce the growth rates at higher k values. d is estimated at 0.05 cm and k_L (as defined in Sec. IV) is $\sim 250\ cm^{-1}$, so that Eq. (48) predicts that the wavenumbers corresponding to maximum growth is in the range $60\ cm^{-1} < k_{MAX} < 250\ cm^{-1}$. The observed periodicities range from $k \sim 60\ cm^{-1}$ to $k \sim 150\ cm^{-1}$. The conditions for the ordinary sausage instability in this current carrying plasma are probably also satisfied in such plasmas;[15] for 200 eV electron temperatures, $B_{self} \sim 10^6$ gauss and $n \sim 10^{20}$, the sausage and flute growth rates are comparable, the sausage growth scaling as $B_n^{-1/2}$ and the flute as $T_e^{1/2}$.

DISCUSSION

In this paper a nonlinear second-order differential equation has been used to analyze the linear onset and nonlinear saturation of a convection instability characteristic of an inhomogeneous plasma in an inhomogeneous magnetic field. This differential-equation approach has been used to extend the frequency range of the usual dispersion-relation analysis to the collisionless limit and the linear stability analysis shows the instability to be the collisional analog of the flute instability, both being driven by a density gradient parallel to a magnetic field gradient. A critical magnetic field, B_c, is predicted, with the plasma becoming unstable when $B > B_c$. When $B < B_c$ the plasma is stabilized by finite gyroradius effects in the collisionless case and by the effect of the mean-free-path in the collisional case. Finite gyroradius corrections to the pressure tensor are also found to be important for large values of the wave vector perpendicular to the

magnetic field.

The form of the nonlinear differential equation indicates that the present instability belongs to a class of instabilities like the Benard instability of a thermally unstable fluid layer and other instabilities that can be described by the equation for an inverted pendulum. These are "symmetry-breaking" zero-frequency instabilities in which a medium that is spatially uniform in the stable state exhibits a periodic spatial structure consisting of convection cells in the unstable state. The ultimate size of such convection cells is determined by a spatial average (over a cell) of the dynamic energy balance, which yields the saturation amplitude of the instability.

The theory of this instability has been applied as a possible additional mechanism to the sausage instability to explain the "beading" effect observed in exploding-wire plasmas, and a thermal-ionization experimental arrangement has been described for the experimental observation of the plasma convection cells.

ACKNOWLEDGMENTS

This research was supported in part by U. S. AFOSR grant AF-76-3129, NSF contracts ENG 76-04635 and MPS 74-12622, and ONR contract NOOO 14-75C-0309-P4.

REFERENCES

*Institute for Physical Science and Technology

1. A. V. Timofeev, Zhur. Tekh. Fig. 33, 776 (1963) [Sov. Phys.-Tech. Phys. 8, 586 (1964)].
2. B. B. Kadomtsev, Plasma Turbulence, Academic Press (New York, 1965) p. 7.
3. N. A. Krall, "Drift Waves", Advances in Plasma Physics, Vol. I, John Wiley and Sons, Inc. (New York, 1971).
4. B. B. Kadomtsev and A. V. Nedospasv, Plasma Phys. 1, 230 (1960).
5. A. Simon, Phys. Fluids 6, 382 (1963).
6. L. Spitzer, Jr., Diffuse Matter in Space, John Wiley and Sons, Inc. (New York, 1968) p. 92.
7. F. Chen, Phys. Fluids 8, 1323 (1965).
8. F. Cap and H. Lashinsky, Nonlinear Vibration Problems (Warsaw) 14, 519 (1973).
9. S. Chandrasekhar, Hydrodynamic and Hydromagnetic Stability, Oxford Press (London, 1961).
10. A. Simon, Phys. Fluids 11, 1186 (1968).
11. M. Rosenbluth, N. Krall, N. Rostoker, Nucl. Fus. Supp., Part I, 143 (1962).
12. M. Rosenbluth and C. Longmire, Ann. Phys. 1, 120 (1957).
13. K. Roberts and J. Taylor, Phys. Rev. Letters 8, 197 (1962).
14. N. Mosher and S. Stephanakis, et al., Ann. N. Y. Acad. Sci. 251, 632 (1975).
15. M. Lampe, et al., to be published.
16. N. Rynn and N. D'Angelo, Rev. Sci. Instr. 31, 1326 (1960).

APPENDIX I

In performing the average over the x dependence to arrive at Eq. (11) a number of numerical factors are encountered. They are defined as:

$$\varepsilon_1 = \int_0^d \frac{\sin \frac{\pi x}{d} \cos \frac{\pi x}{d}}{x} dx \simeq 0.7$$

$$\varepsilon_2 = \int_0^d \frac{(\sin \frac{\pi x}{d})^2}{x} dx \simeq 1.2$$

$$\eta = -\left(1 - \varepsilon_2 - \frac{2\pi\varepsilon_1}{K^2 d^2}\right)$$

or

$$\eta \simeq +\left(0.2 + \frac{4.2}{K^2 d^2}\right)$$

INTERMEDIATE REGIME $\Omega_\alpha >> 1/\tau_\alpha \simeq \lvert\omega\rvert \equiv \lvert\omega_0 + i\gamma\rvert$	
$\gamma =$ $(B \gtrsim B_c)$	$\dfrac{\dfrac{4k^2 T\tau_i}{dRK^2 m_i}\left(1 - \dfrac{B_c^2}{B^2}\right)}{(1+\omega_0^2\tau_i^2)}$
$\omega_0 =$ $(B \gtrsim B_c)$	$\dfrac{2\eta kTc}{eBd}$
$\gamma =$ $(B >> B_c)$	$-\dfrac{1}{2\tau_i} + \dfrac{1}{2}\left(\dfrac{1}{\tau_i^2} + \dfrac{16k^2 T}{dRK^2 m_i}\right)^{1/2}$
$\omega_0 =$ $(B >> B_c)$	0
$\dfrac{eB_c}{m_i c} =$	$\dfrac{K^2 R}{k\tau_i}\left(\dfrac{d}{2R}\right)^{1/2}\left(\dfrac{m_e}{m_i}\right)^{1/4}$
$\dfrac{r_i^2}{d^2} <$ (for instability)	$\dfrac{2v_{thi}^2 k^2 \tau_i^2}{d^3 RK^4}\left(\dfrac{m_i}{m_e}\right)^{1/2}$

TABLE I - Growth rate, γ, frequency, ω_0, and critical magnetic field, B_c, for instability. $K=(k^2+\pi^2/d^2)^{1/2}$ is the total wavenumber, r_i is the ion Larmor radius and v_{thi} is the ion thermal velocity. η is defined in Appendix I.

COLLISIONAL REGIME $\Omega_\alpha >> 1/\tau_\alpha >> \lvert\omega\rvert \equiv \lvert\omega_0 + i\gamma\rvert$	
$\gamma =$ $(B \gtrsim B_c)$	$\frac{4k^2 T \tau_i}{dRK^2 m_i}\left(1 - \frac{B_c^2}{B^2}\right)$
$\omega_0 =$ $(B \gtrsim B_c)$	$\frac{2\eta k T c}{eBd}$
$\gamma =$ $(B >> B_c)$	$\frac{4k^2 T \tau_i}{dRK^2 m_i}$
$\omega_0 =$ $(B >> B_c)$	0
$\frac{eB_c}{m_i c} =$	$\frac{K^2 R}{k\tau_i}\left(\frac{d}{2R}\right)^{1/2}\left(\frac{m_e}{m_i}\right)^{1/4}$
$\frac{r_i^2}{d^2} =$ (for instability)	$\frac{2v_{thi}^2 k^2 \tau_i^2}{d^3 RK^4}\left(\frac{m_i}{m_e}\right)^{1/2}$

TABLE II - Growth rate, γ, frequency, ω_0, and critical magnetic field, B_c, for instability in the collision dominated limit. $K=(k^2+\pi^2/d^2)^{1/2}$ is the total wavenumber, r_i is the ion Larmor radius and v_{thi} is the ion thermal velocity. η is defined in Appendix I.

COLLISIONLESS REGIME $\Omega_\alpha >> \lvert\omega\rvert \equiv \lvert\omega_0 + i\gamma\rvert >> 1/\tau_\alpha$	
$\gamma =$ $(B \gtrsim B_c)$	$\left(\frac{4k^2T}{dRK^2m_i} - \omega_0^2\right)^{1/2}$
$\omega_0 =$ $(B \gtrsim B_c)$	$\frac{\eta kTc}{eBd}$
$\gamma =$ $(B >> B_c)$	$\left(\frac{4k^2T}{dRK^2m_i}\right)^{1/2}$
$\omega_0 =$ $(B >> B_c)$	0
$\frac{eB_c}{m_i c} =$	$\frac{\eta K}{2}\left(\frac{RT}{dm_i}\right)^{1/2}$
$\frac{r_i^2}{d^2} <$ (for instability)	$\frac{4}{\eta^2 K^2 dR}$

TABLE III - Growth rate, γ, frequency, ω_0, and critical magnetic field, B_c, for instability in the collisionless limit. $K = (k^2+\pi^2/d^2)^{1/2}$ is the total wavenumber, r_i is the ion Larmor radius and v_{thi} is the ion thermal velocity. η is defined in Appendix I.

FIGURE CAPTIONS

Fig. 1 Plasma filled gap between two coaxial cylinders of radius R and R+d (R>>d). The azimuthal magnetic field and a local Cartesian coordinate system are shown.

Fig. 2 Plot of growth rate as a function of the axial wavenumber, k. For the case shown here $B>>B_c$ and $T_i=T_e\equiv T$; also $\gamma_{MAX} = -\frac{1}{2\tau_i} + \frac{1}{2}\left(\frac{1}{\tau_i^2} + \frac{16T}{dRm_i}\right)^{1/2}$.

Fig. 3 Plot of growth rate as a function of collision frequency with $k>>\pi/d$. For the case shown here $B>>B_0$ and $T_i=T_e$; also $\gamma_0 = \left(\frac{4T}{dRm_i}\right)^{1/2}$.

Fig. 4 Plot of the critical magnetic field (solid curve) as a function of the axial wavenumber, k, in the collisional regime. The dashed curve separates the regions where the FLR corrections are large and small. The shaded area denotes the region of instability $(\Omega\tau)_i^{MIN} \equiv \left[\frac{2R}{d}\left(\frac{m_e}{m_i}\right)^{1/2}\right]^{1/2}$, $(\Omega\tau_i)^{MAX} \equiv \frac{4d^2}{\pi^2 r_i^2}$, and α is defined in Eq. (33).

Fig. 5 Plot of the critical magnetic field (solid curve) as a function of the axial wavenumber, k, in the collisionless regime. The dashed curve separates the regions where the FLR corrections are large and small. The shaded area denotes the region of instability. τ_N is defined in Eq. (32) and $(\Omega_i\tau_N)^{MAX} \equiv \frac{16d^3}{\sqrt{2}\eta\pi^3 R r_i^2}$.

Fig. 6 Plot of the density as a function of position in the linear stage (labeled by $n^0(x)$) and in the nonlinear stage (labeled by $n_{NL}^0(x)$).

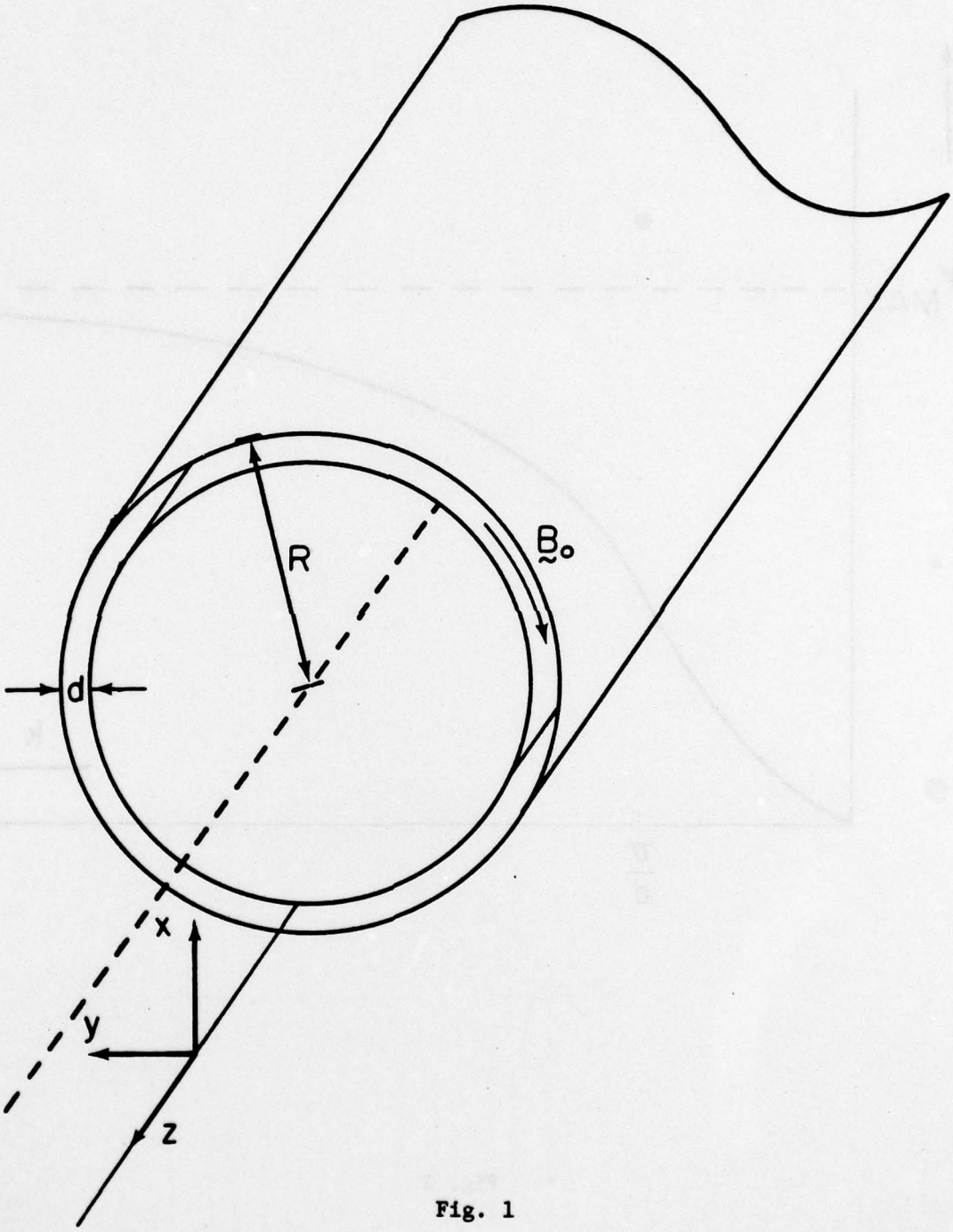

Fig. 1

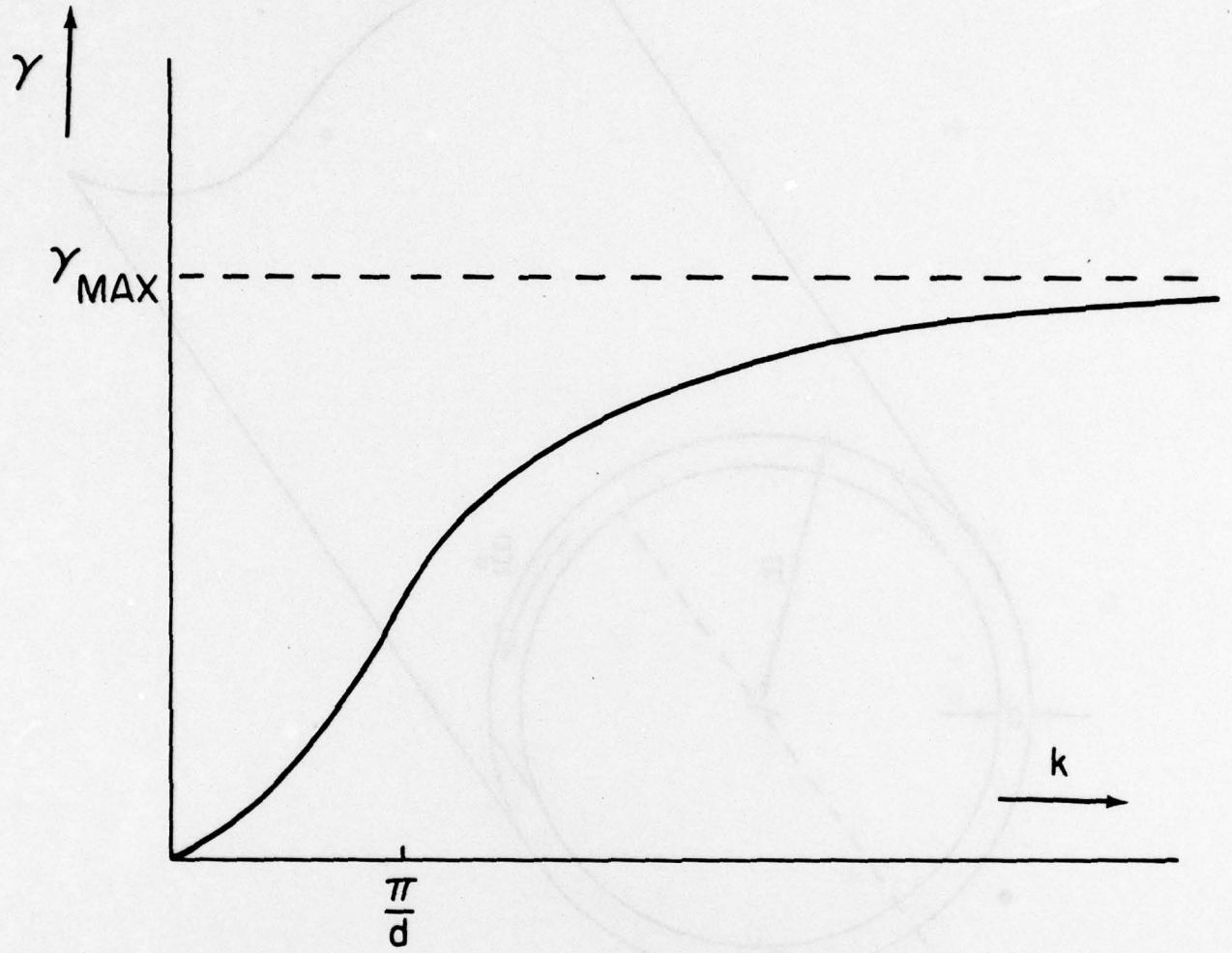

Fig. 2

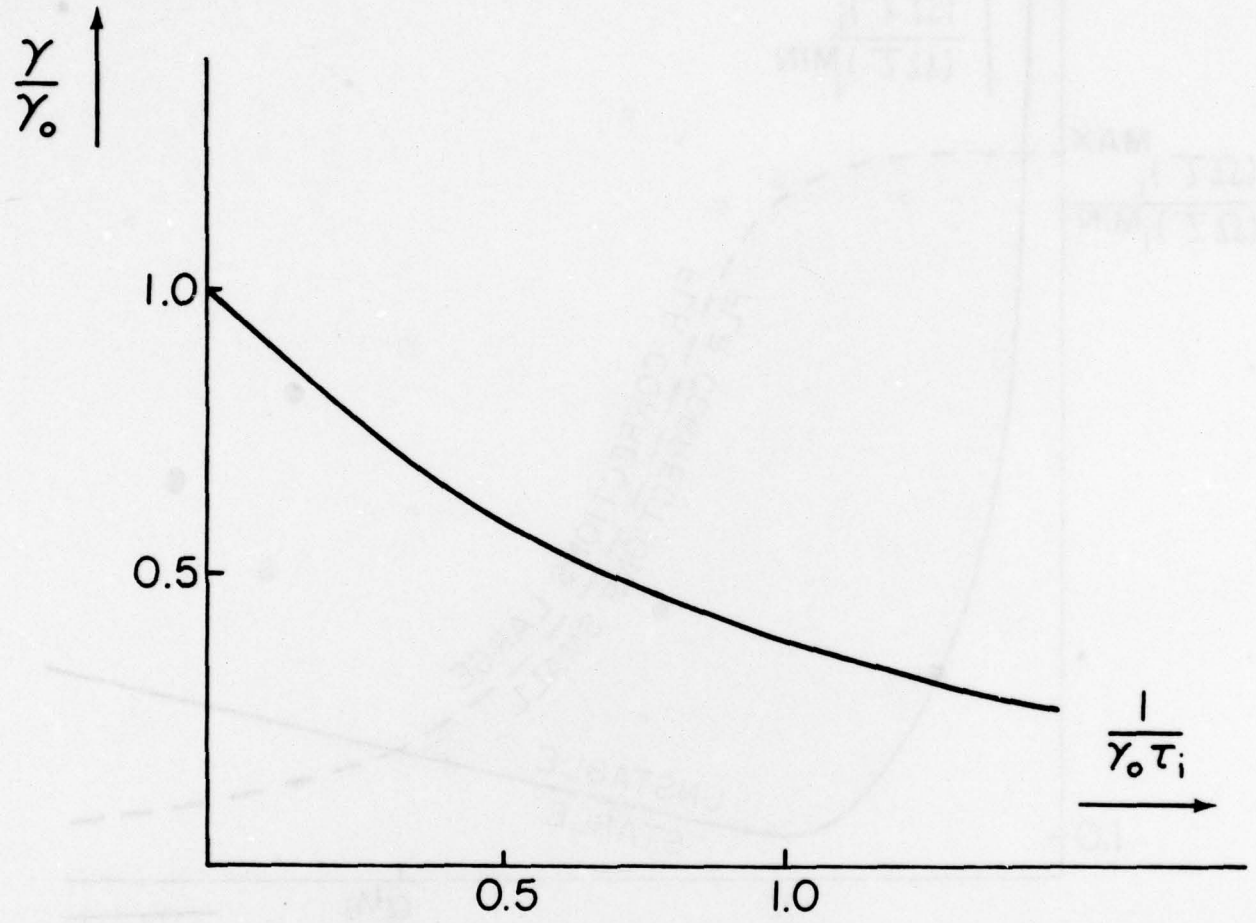

Fig. 3

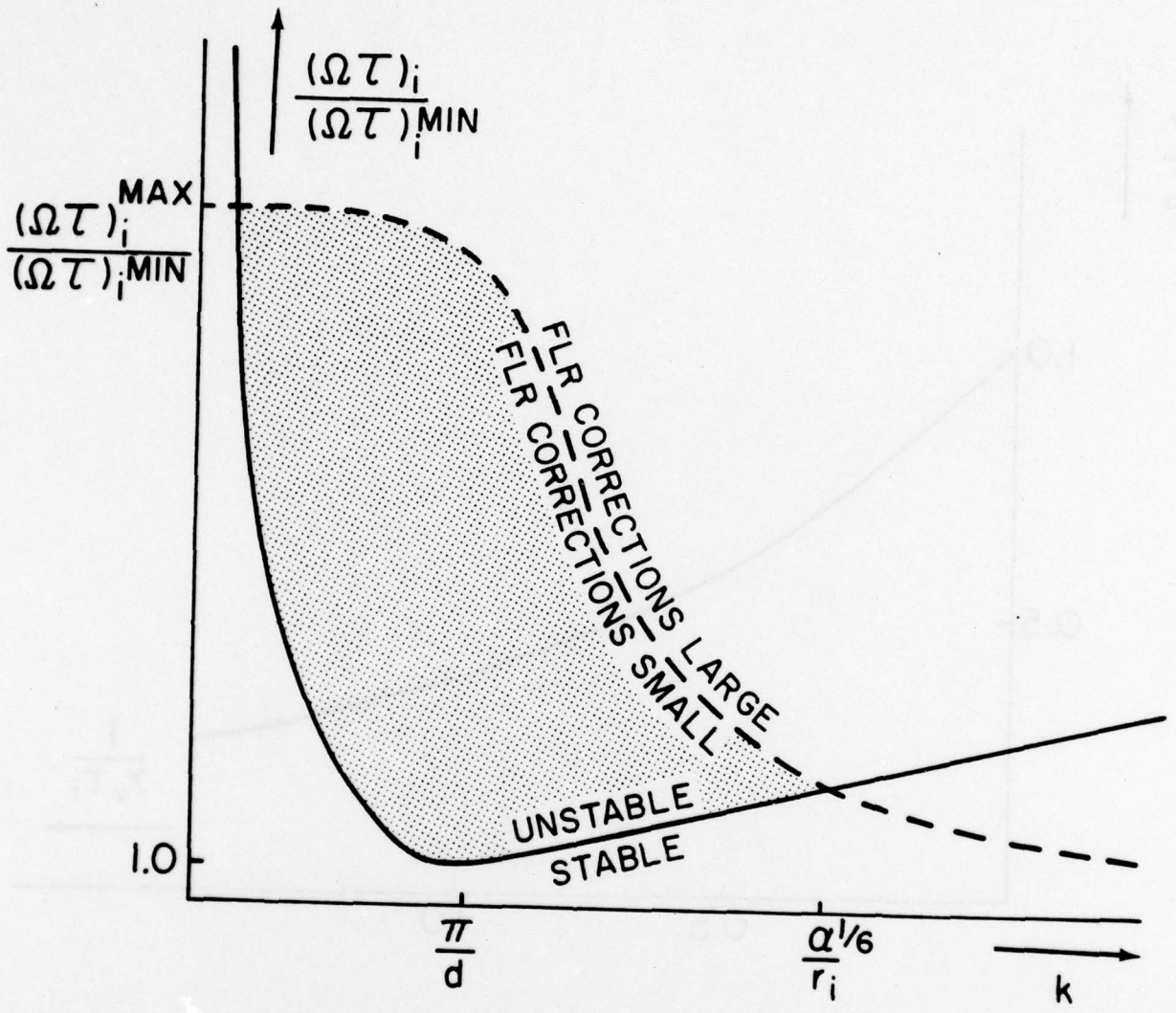
$\frac{(\Omega\tau)_i}{(\Omega\tau)_i^{MIN}}$
$\frac{(\Omega\tau)_i^{MAX}}{(\Omega\tau)_i^{MIN}}$
FLR CORRECTIONS LARGE
FLR CORRECTIONS SMALL
UNSTABLE
STABLE
1.0
$\frac{\pi}{d}$
$\frac{\alpha^{1/6}}{r_i}$
k

Fig. 4

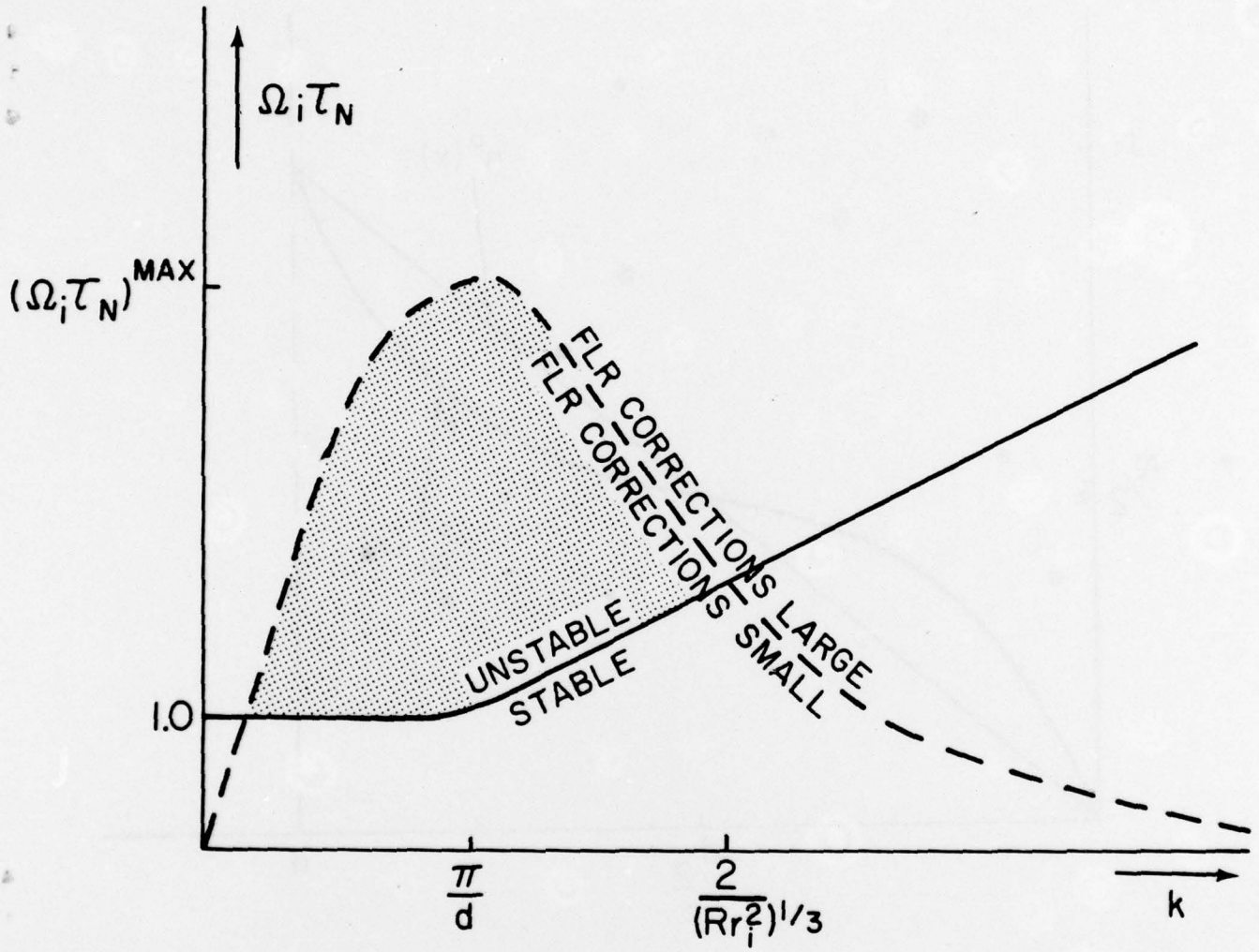
$\Omega_i \tau_N$
$(\Omega_i \tau_N)^{MAX}$
1.0
FLR CORRECTIONS LARGE
FLR CORRECTIONS SMALL
UNSTABLE
STABLE
$\frac{\pi}{d}$
$\frac{2}{(Rr_i^2)^{1/3}}$
k

Fig. 5

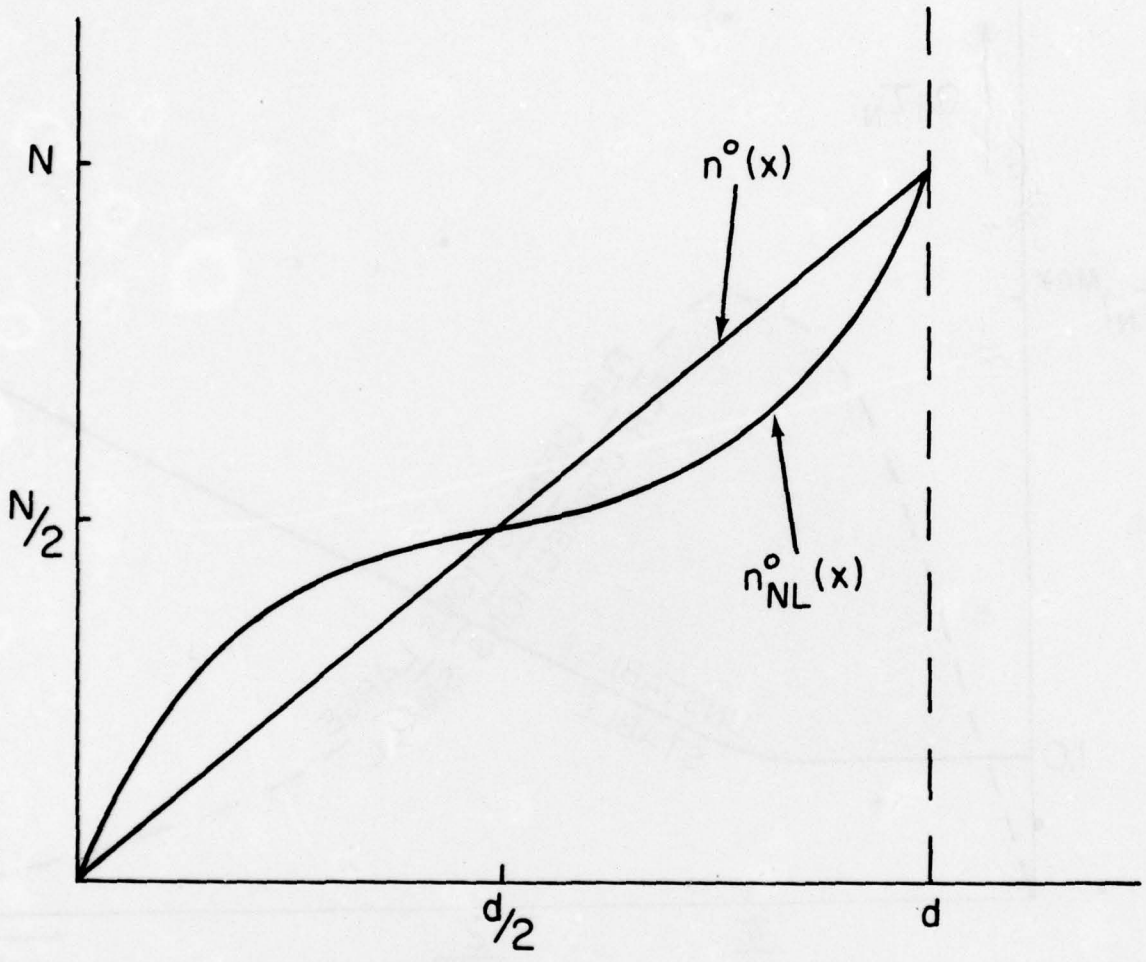

Fig. 6